

# fMRI mapping of a morphed continuum of 3D shapes within inferior temporal cortex

Roger B. H. Tootell<sup>\*†‡§</sup>, Kathryn J. Devaney<sup>\*</sup>, Jeremy C. Young<sup>\*</sup>, Gheorghe Postelnicu<sup>\*</sup>, Reza Rajimehr<sup>\*</sup>, and Leslie G. Ungerleider<sup>\*†¶</sup>

<sup>\*</sup>Martinos Center for Biomedical Imaging, Massachusetts General Hospital, <sup>†</sup>Harvard Medical School, Charlestown, MA 02129; and <sup>‡</sup>Laboratory of Brain and Cognition, National Institute of Mental Health, Bethesda, MD 20892

Contributed by Leslie G. Ungerleider, December 28, 2007 (sent for review December 5, 2007)

Here, we mapped fMRI responses to incrementally changing shapes along a continuous 3D morph, ranging from a head (“face”) to a house (“place”). The response to each shape was mapped independently by using single-stimulus imaging, and stimulus shapes were equated for lower-level visual cues. We measured activity in 2-mm samples across human inferior temporal cortex from the fusiform face area (FFA) (apparently selective for faces) to the parahippocampal place area (PPA) (apparently selective for places), testing for (i) incremental changes in the topography of FFA and PPA (predicted by the continuous-mapping model) or (ii) little or no response to the intermediate morphed shapes (predicted by the category model). Neither result occurred; instead, we found approximately linearly graded changes in the response amplitudes to graded-shape changes, without changes in topography—similar to visual responses in different lower-tier cortical areas.

category | continuous | single-stimulus

In the brains of human and nonhuman primates, object processing involves the inferior temporal (IT) region of the cerebral cortex (1–6). Within this higher-tier region, the fundamental object processing steps appear to be reflected in the functional architecture—just as the functional architecture in lower-tier visual areas reflects the single-unit tuning for ocular dominance, orientation, direction of motion, etc.

Early physiological and optical imaging studies in monkey IT cortex (7–9) proposed that objects are processed according to a continuously changing map of object features, in small cortical columns analogous to those in early visual areas. We refer to this as the “continuous-mapping” model.

Subsequent fMRI research described spatially larger “modules” in human IT cortex, in which specific regions [e.g., the fusiform face area (FFA) and the parahippocampal place area (PPA)] are selectively activated by discrete object categories (i.e., faces and places, respectively) (10–15). This can be called the “category” model of IT organization. Based on functional MRI (fMRI) and single units, apparently homologous category-selective regions and responses have since been reported in monkey cortex (16–19). Empirically, the sheer number of fMRI reports for such modular regions is very persuasive—but competing possibilities have been proposed (20–22). Here, we systematically tested and compared these two models, using a fMRI approach.

In previous fMRI studies, object selectivity has typically been tested by comparing multiple, naturalistic images of objects from a given object category versus multiple, naturalistic images from control category(ies). This approach can make it difficult to tease apart underlying effects. For example, use of multiple images makes it impossible to map the fMRI activity evoked by each single image within the category; group-common differences (e.g., according to category) are all that can be demonstrated by such an approach. Similarly, use of naturalistic images makes it difficult to study the effect of incremental changes in shape (as in lower-tier studies of orientation and direction), because naturalistic stimuli are not easily manipulated. With

naturalistic images, it is also difficult to disambiguate the effects of shape from those due to variations in surface reflectance features (e.g., texture, luminance, color, specular reflection, etc.).

Here, we used stimuli that avoid all of these problems. Activity was mapped independently in response to each single stimulus shape (“single-stimulus imaging”), using extensive signal averaging. Experimental stimuli were computer-generated, 3D morph shapes. These shapes had a uniform surface reflectance and were equated for surface volume and closely matched for averaged retinotopic extent. The two extremes of the morph continuum (an *en face* view of a head versus a house; i.e., a face and a place) belonged to neuropsychologically relevant categories that are reportedly mapped in different cortical locations (13, 14). However, the morph stimuli also included geometrically intermediate shapes that belonged to no identifiable object category (things). Instead of supporting either the category model or the continuous-mapping model, our results were best fit by a different model typical of the organization in lower-tier visual cortical areas.

## Results

**Conventional Localizers.** First, we did control scans to localize areas FFA and PPA in each subject, using conventional blocks of multiple, naturalistic stimuli (faces versus places), during central fixation. Here, the retinotopic boundaries and stimulus features (clutter, spatial frequency) were equated or closely matched, and signal averaging was extensive.

Fig. 1 shows maps of the resultant activity. Fig. 1*A* appears very similar to previously published maps; it shows FFA and PPA in their expected locations, as spatially separated regions of face- and place-selective activity. However, to topographically isolate FFA and PPA in this extensively averaged data, we had to increase the statistical threshold to extremely high levels ( $P < 10^{-55}$ ). When the threshold was instead lowered to more traditional levels (Fig. 1*B*;  $P < 10^{-5}$ ), we found that the face- and place-selective regions (i.e., FFA and PPA) actually adjoin each other—even without spatial filtering.

The main goal of the present study was to measure incremental changes in fMRI activity across cortex, from FFA through PPA (e.g., along the red line in Fig. 1*A* and *B*), in response to correspondingly incremental changes in stimulus shape. Fig. 1

Author contributions: R.B.H.T. and L.G.U. designed research; K.J.D., J.C.Y., and R.R. performed research; G.P. contributed new reagents/analytic tools; K.J.D. and J.C.Y. analyzed data; and R.B.T. wrote the paper.

The authors declare no conflict of interest.

Freely available online through the PNAS open access option.

<sup>§</sup>To whom correspondence may be addressed at: Martinos Center for Biomedical Imaging, Massachusetts General Hospital, 149 13th Street, Charlestown, MA 02129. E-mail: tootell@nmr.mgh.harvard.edu.

<sup>¶</sup>To whom correspondence may be addressed. E-mail: ungerlel@mail.nih.gov.

This article contains supporting information online at [www.pnas.org/cgi/content/full/0712274105/DC1](http://www.pnas.org/cgi/content/full/0712274105/DC1).

© 2008 by The National Academy of Sciences of the USA

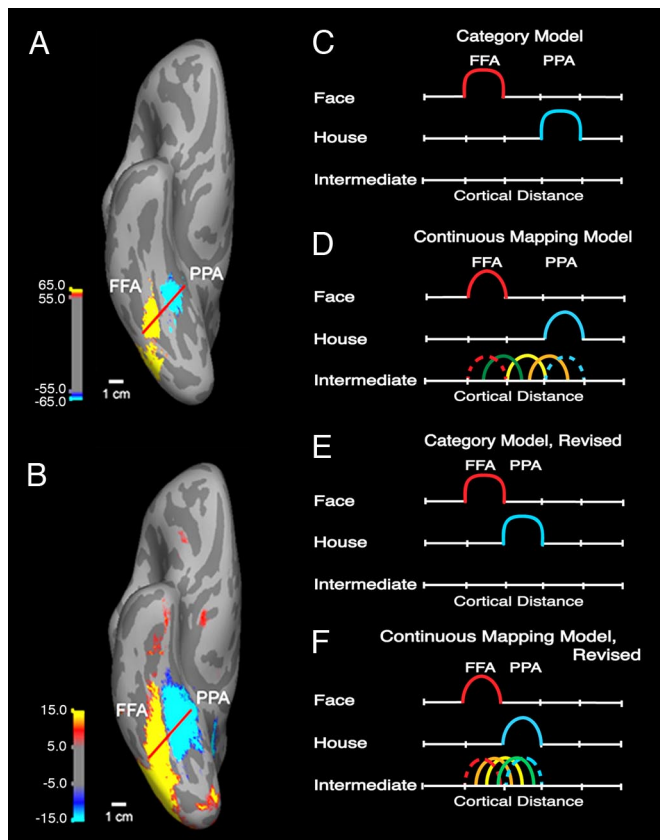


**Fig. 1.** Response predictions to the present morph stimuli based on two models and two assumptions about the FFA/PPA topography. (A and B) Identical data are shown, at high and standard statistical thresholds, respectively. The pseudocolor scale indicates the exponent of a random-chance probability; thus, the probability of achieving a similar result by random chance is  $<10^{-55}$  (A) and  $10^{-5}$  (B). The data are a group ( $n = 10$ ) average on the cortical surface, based on 12,096 functional volumes of fMRI data, in block-design comparisons of naturalistic images of faces and places. The peaks of activity (A) in FFA and PPA are topographically separated by 9 mm. However, at lower threshold (B), the face- and place-biased regions border each other. (C–F) Two models' predictions to the morph stimuli, along a sampling line along the cortical surface spanning FFA and PPA (indicated by the red line in A and B). Models are described for two scenarios; one in which PPA and FFA are adjacent (as found here) and another in which these two areas are topographically separated (as described in some previous studies). The predictions of the model are similar in these two scenarios but without a topographical gap in the former (compare C and D with E and F). Across the cortical surface (x axis), both models predict high activity to the face in FFA (red), and high activity to the house in PPA (cyan). The continuous-mapping model predicts a shift in the peak location of fMRI activity, between FFA and PPA, as shape is varied between the two morph extremes. The category model predicts no such shift; instead, its distinctive feature is a lack of activity to the intermediate morph shapes. Here, the shape of the predicted activity topography is also slightly different: The category model predicts a topographically flat, high sensitivity to faces everywhere in FFA, without falloff except for that imposed by the spatial resolution limits of the fMRI. The continuous map predicts a more Gaussian topography—reflecting an optimal stimulus that is represented one column wide and progressively less-optimal stimuli coded in adjoining columns—slightly blurred by the fMRI.

C–F shows the most stringent predictions of the two main models, when measured along such sampling lines.

**Main (Morph) Experiment.** Fig. 2 shows the morph stimuli. One extreme of the morph continuum was a 3D rendering of a head, viewed slightly off-center. The other extreme was a house, viewed from a similar vantage point. Between these two morph extremes, 3D shape varied continuously, based on linearly proportionate

changes along 3D distance functions. To optimize statistical sensitivity, the five representative shapes (at 25% steps along the morph continuum, indicated by blue boxes in Fig. 2) were presented by using one shape per block. Thus, in each block, we measured the fMRI activity in response to a single shape at a constant viewpoint, size, and position. To refresh neural activity within each (randomly ordered) common-shape block, the location of the virtual light source was changed every 2 seconds, systematically and equivalently, for each morph shape. This variation in illuminant position effectively eliminated repetition suppression.

Consistent with previous studies using naturalistic stimuli, the morph-based face and house shapes (i.e., 100/0% in Fig. 2) produced relatively higher activity in FFA and PPA, respectively [see supporting information (SI) Fig. 7]. Fig. 3 shows the grid-based region-of-interest (ROI) analysis used to measure the detailed activity in these two areas, and the cortical region between them, in each subject. As in Fig. 1B, the morph-driven regions FFA and PPA in Fig. 3 are topographically adjacent, without activity gaps between them.

According to the most stringent version of the category model (Fig. 1 C and E), the face and house shapes should produce robust fMRI activity in their respective areas—but the intermediate morph shapes should produce little or no activity, because those shapes do not belong to any object category. Instead, we found that those noncategorical, intermediate shapes produced at least as much activity as the recognizable, categorical face and house (see Fig. 4). Thus, that prediction of the category model was not fulfilled.

According to the continuous-mapping model, the peak of cortical activity should shift gradually across cortex, between FFA and PPA, because the stimulus shape is changed accordingly (Fig. 1 D and F). However, we found that the predicted topographical shift did not occur, within the sampled region in either single subjects (see SI Fig. 8) or the average across subjects (Fig. 5). Thus, the continuous-mapping idea was not confirmed, in general. Instead, the amplitude of activity scaled up or down with the shape changes, in a graded manner without discontinuity between recognizable and unrecognizable shapes. Although there was a trend for activity to shift systematically in the correct direction within FFA (see Fig. 5), the size of this topographic shift was only 20% of that predicted by the continuous-mapping model, and there was no analogous shift within PPA—so presumably this is noise.

**Attention Control.** One possible concern is whether uncontrolled attention affected the above results, e.g., because of the differences in shape recognizability. To stabilize attention during scanning, we had subjects detect the presence of a briefly presented dot, which could occur anywhere on the morph shapes during scanning, at unpredictable times. The detectability of the dot converged to 67% correct, based on a staircase modulation of dot luminance relative to the local background luminance (as in refs. 23 and 24). This attention manipulation did not significantly change the topography of our fMRI data (see SI Figs. 9–11). Thus, the fMRI activity in our other measurements appears to be driven, at least largely, by sensory (rather than higher-order) aspects of the stimuli, as in the initial descriptions of FFA and PPA (13, 25).

## Discussion

This study was designed to quantitatively compare two widely discussed models of the functional organization in IT cortex.

**Continuous-Mapping Model.** One model of IT architecture (8) is an extension of the well known columnar architecture described in early visual areas. In this continuous-mapping model, each specific visual feature is an optimal stimulus for a given corresponding column, less than a millimeter in width. Similar visual features activate adjoining columns. Thus, as one moves across the cortical surface, the optimal stimulus for the underlying

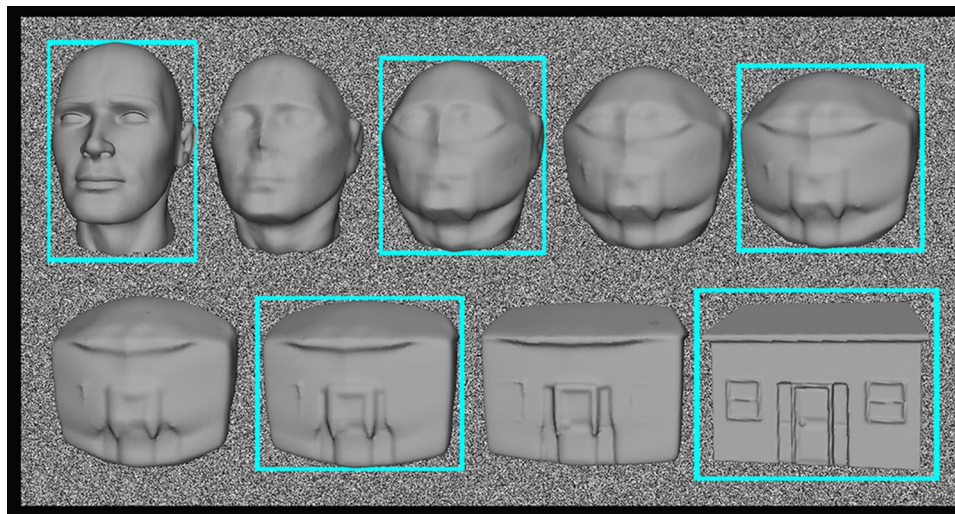


**Fig. 2.** Representative shapes along the morph continuum. The five shapes tested in this study are enclosed in cyan rectangles. In the experiment, the cyan rectangles were not present, and a small central fixation cross was included throughout the scan.

neurons will continue to change until the “best” feature becomes progressively quite different from the original feature—and resolvable by fMRI. In this way, one could end up with two regions that respond optimally to faces and places.

The continuous-mapping model has not been formally tested with fMRI, to our knowledge. However, this model is supported by anecdotal reports that different face stimuli produce a slightly different (although overlapping) pattern of cortical activation in both macaques (18) and humans (26). That is, the different features in each set of faces produce a slightly different topography of activation.

Generally, our results did not support the continuous-mapping model (see Figs. 1*D* and *F*, and 5). To a first approximation, the peak of activity remained in either FFA or PPA; it did not shift continuously across the cortical surface as the shape changed accordingly. One could instead imagine that a continuous topographical shift did occur but in a way that was not captured by our rectangular ROIs. However, we did examine the maps in great detail and found no evidence for such irregular topographical shifts in either the grouped or the individual activity maps.

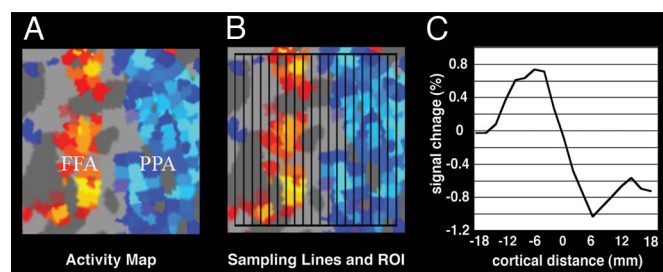


**Fig. 3.** Region-of-interest (ROI) tests of the morph data. (A) A magnified topographical view of the activity in FFA and PPA from one subject’s hemisphere, in response to the two extremes of the morph continuum. Relatively higher activity in response to the morphed face is shown in yellow/red, and higher activity to the house is shown in cyan/blue. As in *B*, a rectangular-shaped ROI was placed over these two areas, with the midline aligned on the border between PPA and FFA. Within this ROI, we sampled within strips 2 mm wide. (C) Results of this analysis, for the comparison [face minus house]. As described in Fig. 1*B*, FFA and PPA border each other directly: If there were instead a region of inactivated cortex between these two functional regions, it would show up as a flat (horizontal) line segment in this function, interspersed midway between FFA and PPA.

**Category Model.** In contrast, the category model (Fig. 1*C* and *E*) assumes that FFA and PPA are primarily activated by stimuli belonging to a given object category (faces and places, respectively). By this model, intermediate morph shapes should produce little or no activity, because these shapes do not belong to any object category. That prediction was also not met here; intermediate morph shapes instead produced levels of activity that were equal to that produced by the face and house.

Alternatively, it has been argued that FFA reflects the effects of expertise (20). However, such an influence of expertise was not evident here (e.g., Fig. 4). In contrast to the face and house shapes, subjects had never seen the intermediate shapes before the experiment, and did not actively discriminate those intermediate shapes during the experiment. Nevertheless all shapes produced equally robust activity.

**“Norm-Based” Model.** Recent single-unit and fMRI studies (15, 27, 28) have suggested an alternative model. In this norm-based model, exemplars of a given category are represented based on their distance from a learned object mean (the norm), and neural responses increase with increasing distance from that mean. Presumably that model would predict slight increases in FFA or PPA responses to faces or houses (respectively) that were slightly different (e.g., 95/5%) from the norm-based exemplars used here (100/0%). However, that model is ultimately a within-category model, which makes no explicit prediction for the between-category results described here.

**“Different-Area” Model.** In both human and nonhuman subjects, the morph data suggest an alternative model (Fig. 6), which (for lack of a better name) we call the different-area model. This model is analogous to the relationship between areas MT and V4, which lie adjacent to each other at lower levels of the visual cortex: certain visual stimuli (e.g., moving stimuli) preferentially activate area MT, whereas different visual stimuli (e.g., stationary flashed bars) produce relatively higher activation in V4 (e.g., refs. 29–34). By analogy, the present results suggest that specific regions of IT cortex (e.g., the different areas FFA and PPA) are functionally distinguishable from each other, and from other cortical regions without strictly defining the exact optimal stimuli and without assuming that higher-order cognitive influences (e.g., meaning, context) have any prominent effect (as in the current category model).



## Experimental Procedures

**Visual Stimuli.** Morph shapes were calculated by representing the two end shapes (head/face and house) implicitly as signed distance functions in the 3D domain. After that, the continuous morph was computed so as to minimize the pointwise difference between the distance functions in the 3D domain while preserving at each intermediate point a solution that represented a signed distance function. For more details, see ref. 37.

Stimuli were presented in the scanner via LCD projector (Sharp XG-P25, resolution = 1,024 × 768; screen size ≈ 31 × 23°), by using MacStim Presentation. All morph shapes were equated for volume, surface reflectance, center location, virtual distance from the viewer, and viewpoint (relative to the “frontal” viewpoint defined for the two extreme shapes). In a block design, five test shapes were chosen, at 25% steps along the morph dimension. Each of the five shapes was presented unchanged throughout a given block, except as follows. To “refresh” fMRI activity within a block, the location of the (single) virtual light source was systematically varied every second. To minimize retinotopic artifacts, each of the five shapes was presented on a random dot background, and the individual random dot arrays were rerandomized at every change in shape or lighting (i.e., every second). Blocks devoted to each shape were presented in semirandom order. Also included in each scan were baseline blocks of uniform gray and blocks of grid-scrambled images.

**Imaging Procedure.** Subjects were scanned in a 3T MRI (TIM Trio; Siemens), using a single-shot gradient echo EPI sequence. Subjects fixated a central fixation cross that was present on all images. From each of five subjects, 15,360 functional volumes were obtained (33 slices, voxels 3 × 3 × 3 mm, TR 2 sec). All human subjects gave written consent, and the experimental protocol was approved by the Massachusetts General Hospital Institutional Review Board. All subjects had normal or corrected-to-normal vision. High-resolution 3D anatomical MR images (MP-RAGE) were also acquired from each subject, for use in subsequent cortical reconstruction cortex in flattened format (38, 39).

**Attention Control.** To control for variations in attention, additional experiments were conducted in which the subjects performed a detection task

during presentation of all shapes. Subjects used in the attention control were also subjects in the passive-viewing experiments.

In this condition, each subject was cued (by the stimulus image change, once per second) to respond (via a button box located inside the scanner) by pressing button 1 if a small (0.2° × 0.2°) red probe dot was present in the shape and button 2 if it was absent. The probe dot was present in 50% of the shapes, randomly ordered. When present, the probe dot could appear anywhere in the shape, with equal spatial probability. Thus, to achieve optimal performance, subjects had to attend carefully to the full visuotopic extent of each shape.

The detectability of the probe dot was manipulated by varying its red/white ratio (decreased saturation = decreased detection). Because the white value varied over the shape (due to changes in lighting and local surface curvature), that value was always made equal to the average of the pixel group that it replaced on each image. Threshold was modulated by the staircase method (converging on 68% correct), to keep subjects' performance level constant, and to prevent pop-out effects. The subjects' performance was thus equated across the different shape conditions.

**Data Analysis.** Data were analyzed by FS-FAST and FreeSurfer (<http://surfer.nmr.mgh.harvard.edu>). All functional images were motion-corrected (40), spatially smoothed with a Gaussian kernel of 2.5 mm (HWHM), and normalized across sessions individually. Average signal intensity maps were calculated for each condition, for each individual subject. Voxel-by-voxel statistical tests were conducted by computing contrasts based on a univariate general linear model. Significance levels were projected onto the flattened cortex individually and computed by using a fixed-effects model. For averaging across subjects, each subject's functional and anatomical data were spatially normalized by using the spherical transformation (38, 39).

**ACKNOWLEDGMENTS.** We thank Aurora I. Ramos and Olivia Wu for help with the figures and Hauke Kolster for significant help with Matlab coding. This work was supported by National Institutes of Health Grants R01 MH67529 and R01 EY017081 (to R.B.H.T.) and P41 RR14075, grants from the MIND Institute, and generous support from the Athinoula A. Martinos Center for Biomedical Imaging. L.G.U. was supported by the National Institute of Mental Health Intramural Research Program.

- Bruce C, Desimone R, Gross CG (1981) Visual properties of neurons in a polysensory area in superior temporal sulcus of the macaque. *J Neurophysiol* 46:369–384.
- Kanwisher N, Chun MM, McDermott J, Ledden PJ (1996) Functional imaging of human visual recognition. *Brain Res Cogn Brain Res* 5:55–67.
- Kourtzi Z, Kanwisher N (2001) Representation of perceived object shape by the human lateral occipital complex. *Science* 293:1506–1509.
- Kreiman G, et al. (2006) Object selectivity of local field potentials and spikes in the macaque inferior temporal cortex. *Neuron* 49:433–445.
- Malach R, et al. (1995) Object-related activity revealed by functional magnetic resonance imaging in human occipital cortex. *Proc Natl Acad Sci USA* 92:8135–8139.
- Sergent J, Ohta S, MacDonald B (1992) Functional neuroanatomy of face and object processing. A positron emission tomography study. *Brain* 115(Pt 1):15–36.
- Fujita I, Tanaka K, Ito M, Cheng K (1992) Columns for visual features of objects in monkey inferotemporal cortex. *Nature* 360:343–346.
- Tanaka K (1996) Inferotemporal cortex and object vision. *Annu Rev Neurosci* 19:109–139.
- Wang G, Tanaka K, Tanifuji M (1996) Optical imaging of functional organization in the monkey inferotemporal cortex. *Science* 272:1665–1668.
- Martin A, Wiggs CL, Ungerleider LG, Haxby JV (1996) Neural correlates of category-specific knowledge. *Nature* 379:649–652.
- Avidan G, Hasson U, Malach R, Behrmann M (2005) Detailed exploration of face-related processing in congenital prosopagnosia: Functional neuroimaging findings. *J Cogn Neurosci* 17:1150–1167.
- Downing PE, Jiang Y, Shuman M, Kanwisher N (2001) A cortical area selective for visual processing of the human body. *Science* 293:2470–2473.
- Epstein R, Kanwisher N (1998) A cortical representation of the local visual environment. *Nature* 392:598–601.
- Kanwisher N, McDermott J, Chun MM (1997) The fusiform face area: A module in human extrastriate cortex specialized for face perception. *J Neurosci* 17:4302–4311.
- Loffler G, Yourganov G, Wilkinson F, Wilson HR (2005) fMRI evidence for the neural representation of faces. *Nat Neurosci* 8:1386–1390.
- Kiani R, Esteky H, Mirpour K, Tanaka K (2007) Object category structure in response patterns of neuronal population in monkey inferior temporal cortex. *J Neurophysiol* 97:4296–4309.
- Pinsk MA, DeSimone K, Moore T, Gross CG, Kastner S (2005) Representations of faces and body parts in macaque temporal cortex: A functional MRI study. *Proc Natl Acad Sci USA* 102:6996–7001.
- Tsao DY, Freiwald WA, Knutsen TA, Mandeville JB, Tootell RB (2003) Faces and objects in macaque cerebral cortex. *Nat Neurosci* 6:989–995.
- Tsao DY, Freiwald WA, Tootell RB, Livingstone MS (2006) A cortical region consisting entirely of face-selective cells. *Science* 311:670–674.
- Gauthier I, Tarr MJ, Anderson AW, Skudlarski P, Gore JC (1999) Activation of the middle fusiform ‘face area’ increases with expertise in recognizing novel objects. *Nat Neurosci* 2:568–573.
- Haxby JV, et al. (2001) Distributed and overlapping representations of faces and objects in ventral temporal cortex. *Science* 293:2425–2430.
- Ishai A, Ungerleider LG, Martin A, Schouten JL, Haxby JV (1999) Distributed representation of objects in the human ventral visual pathway. *Proc Natl Acad Sci USA* 96:9379–9384.
- Sasaki Y, et al. (2006) The radial bias: A different slant on visual orientation sensitivity in human and nonhuman primates. *Neuron* 51:661–670.
- Sasaki Y, Vanduffel W, Knutsen T, Tyler C, Tootell R (2005) Symmetry activates extrastriate visual cortex in human and nonhuman primates. *Proc Natl Acad Sci USA* 102:3159–3163.
- Kanwisher N (2003) The ventral visual object pathway in humans: Evidence from fMRI. *The Visual Neurosciences*, Chalupa L, Werner J, eds (MIT Press, Cambridge, MA), pp 1179–1189.
- Malach R, Levy I, Hasson U (2002) The topography of high-order human object areas. *Trends Cogn Sci* 6:176–184.
- Kayaert G, Biederman I, Op de Beeck HP, Vogels R (2005) Tuning for shape dimensions in macaque inferior temporal cortex. *Eur J Neurosci* 22:212–224.
- Leopold DA, Bondar IV, Giese MA (2006) Norm-based face encoding by single neurons in the monkey inferotemporal cortex. *Nature* 442:572–575.
- Albright TD, Desimone R, Gross CG (1984) Columnar organization of directionally selective cells in visual area MT of the macaque. *J Neurophysiol* 51:16–31.
- Desimone R, Schein SJ (1987) Visual properties of neurons in area V4 of the macaque: sensitivity to stimulus form. *J Neurophysiol* 57:835–868.
- Desimone R, Schein SJ, Moran J, Ungerleider LG (1985) Contour, color and shape analysis beyond the striate cortex. *Vision Res* 25:441–452.
- Maunsell JH, Van Essen DC (1983) Functional properties of neurons in middle temporal visual area of the macaque monkey. Selectivity for stimulus direction, speed, and orientation. *J Neurophysiol* 49:1127–1147.
- Tanaka M, Weber H, Creutzfeldt OD (1986) Visual properties and spatial distribution of neurones in the visual association area on the prelunate gyrus of the awake monkey. *Exp Brain Res* 65:11–37.
- Zeki SM (1974) Functional organization of a visual area in the posterior bank of the superior temporal sulcus of the rhesus monkey. *J Physiol* 236:549–573.
- O'Craven KM, Downing PE, Kanwisher N (1999) fMRI evidence for objects as the units of attentional selection. *Nature* 401:584–587.
- Wojciulik E, Kanwisher N, Driver J (1998) Covert visual attention modulates face-specific activity in the human fusiform gyrus: fMRI study. *J Neurophysiol* 79:1574–1578.
- Chariat G, Faugeras O, Keriven R (2005) Approximations of shape metrics and applications to shape warping and empirical shape statistics. *J Soc Found Comp Math* 5:1–58.
- Dale AM, Fischl B, Sereno MI (1999) Cortical surface-based analysis. Segmentation and surface reconstruction. *NeuroImage* 9:179–194.
- Fischl B, Sereno MI, Dale AM (1999) Cortical surface-based analysis. Inflation, flattening, and a surface-based coordinate system. *NeuroImage* 9:195–207.
- Cox RW, Jesmanowicz A (1999) Real-time 3D image registration for functional MRI. *Magn Reson Med* 42:1014–1018.